Hebron Project Report Cover:Layout 1 6/7/10 3:10 PM Page 1

Hebron

HEBRON PROJECT

Comprehensive Study Report
Offshore Spill Trajectory Modelling Report
February 2011

ExxonMobil Chevron SUNCOR ENERGY Statoil nalcor energy

Prepared for:
Stantec Consulting Ltd.

Results from Simulations of Oil Spills at the Hebron Well Site

ASA Project 2010–261 **February 2011**

Prepared by:

Chris Galagan
Nicholas Cohn
Rachel Shmookler



Applied Science Associates, Inc.
55 Village Square Drive
South Kingstown, RI 02879

Executive Summary

The SIMAP oil spill model was used to simulate spills of crude and fuel oil spills at the Hebron offshore site southeast of St. John's, Newfoundland. The model scenarios use wind data obtained from model hindcasts and field measurements, current data from multiple hydrodynamic models and ice data from the Canadian Ice Service. The SIMAP model was used in stochastic and deterministic modes to determine the range of possible water surface oiling, oil in the water column and shoreline oiling predicted to occur in both summer and winter season conditions. This report describes the wind, current and ice data used in the modeling, it also describes the models applied to simulate the hydrodynamics and the oil spills, and presents and discusses the model results.

Possible spills at the site of the Hebron platform include crude oil from a well blow-out, either at the seabed or from the top of the drilling platform with durations of 30 to 120 days. Short-duration (24 hours or less) small volume batch spills of crude oil and marine diesel fuel were also modeled. All spill scenarios are simulated without any spill countermeasures applied.

Wind data for the oil spill simulations were obtained from two sources. One source is the MSC50 Wind Hindcast, a model reanalysis product that provides hindcast winds for the north Atlantic for the period 1954 through 2008. The data were supplied by Environment Canada, MSC Atlantic Operations. Additional wind data were obtained from the National Centers for Environmental Prediction (NCEP) at multiple locations across the north Atlantic. Oil spill simulations were run using summer and winter season winds in order to capture seasonal differences.

Currents for the North Atlantic region were acquired from the HYCOM (HYbrid Coordinate Ocean Model) circulation model. Hindcast currents from the HYCOM model were obtained for the period November 2003 through September 2010 for the North Atlantic region and used in the SIMAP oil spill model to simulate spills originating at the Hebron platform and from the subsea blow-out.

Ice data used in the oil spill model simulations were obtained from the National Snow and Ice Data Center (http://nsidc.org/index.html) for the months of February and March. Data from the 1989-1990 winter were selected because they show the greatest extent of ice coverage over the past several decades.

The SIMAP stochastic model was used to determine the probability of oiling the water surface and the shoreline based on specified thickness thresholds, and of oiling the water column using a concentration threshold. The following thresholds were applied:

- Surface oil average thickness > 0.01 mm (10 µm)
- Shoreline oil average thickness > 0.01 mm (10 µm)
- Entrained oil (in water column) average > 10 ppb

The majority of spills at the site are predicted to travel eastward. The distance traveled is generally controlled by the blow-out duration and the season. Winter winds on average blow at a higher velocity resulting in greater oil transport. A subset of the summer and winter blow-out

spill simulations of greater than 30 days duration are predicted to reach segments of the Newfoundland shoreline.

Similar to the blow-outs of crude oil, marine diesel and crude oil released in batch transfer spills is predicted to travel primarily toward the east away from Newfoundland. The marine diesel fuel is more easily dispersed into the water column than the crude oil and modeling predicts slightly higher entrained oil fractions for these spills. The marine diesel is capable of achieving a smaller minimum thickness than the crude oil, resulting in a relatively higher sea surface area exposed to oil. None of the batch transfer spills are predicted to reach the Newfoundland shoreline.

Summary Table

Spill	% Water Surface	% Evaporated	% Decayed	% Water Column
Platform Blow-outs	51% to 79%	8% to 12%	12% to 37%	0.2% to 0.3%
Subsea Blow-outs	29% to 35%	29% to 32%	26% to 30%	9% to 10%
Marine Diesel Batch Transfer	0%	6% to 45%	15% to 24%	40% to 70%
Crude Batch Transfer	64%	12% to 13%	22% to 23%	0.4% to 0.5%

Table of Contents

Executive Summary ii
Table of Contents iv
List of Figures v
List of Tables vi
1. Introduction 1
2. Model Inputs and Spill Scenarios 1
  2.1 Study Area 1
  2.2 Model Scenarios 2
  2.3 Oil Characterization 3
  2.4 Wind Data 4
  2.5 Current Data 6
  2.6 Ice Data 7
3. Modeling Description 11
  3.1 Blow-outs of Crude Oil 11
    Blow-outs 11
    Blow-out Plume Dynamics 13
4. Model Results 14
  4.1 Stochastic Model Results 14
  4.2 Deterministic Model Results 16
  4.3 Newfoundland Shoreline Oiling 19
6. References 20
Appendix A: SIMAP Model Description 1
Appendix B: Blow-out Model Description 1
Appendix C: Stochastic Model Results 1
Appendix D: Deterministic Model Results 1

List of Figures

Figure 2.1-1. Map showing the Newfoundland region. 2
Figure 2.4-1. Map showing the locations of wind data stations for the offshore modeling. 4
Figure 2.4-2. Wind rose of the MSC50 wind data from site M6010632 near the Hebron platform location for all months of the year. The plot indicates the direction from which the wind is coming for the 30 years 1976 through 2008. 5
Figure 2.4-3. Wind rose of the MSC50 wind data from site M6010632 near the Hebron platform location for winter months. The plot indicates the direction from which the wind is coming for the 30 years 1976 through 2008. 5
Figure 2.4-4. Wind rose of the MSC50 wind data from site M6010632 near the Hebron platform location for summer months. The plot indicates the direction from which the wind is coming for the 30 years 1976 through 2008. 6
Figure 2.5-1. Map of the large scale ocean currents in the Newfoundland region. (Source: U.S. Coast Guard, International Ice Patrol). 7
Figure 2.6-1. Total accumulated ice coverage for the period of record from the Canadian Ice Service. 8
Figure 2.6-2. Ice concentration chart form the Canadian Ice Service for the week of 12 March, 1990. 9
Figure 2.6-3. Sea ice coverage used in the oil spill model simulations for the month of February. 10
Figure 2.6-4. Sea ice coverage used in the oil spill model simulations for the month of March. . 11
Figure 3.2-1. Perspective view of example oil/gas plume reaching termination depth. 12

List of Tables

Table 2.2-1. Oil spill scenarios modeled at the Hebron Platform location. 3
Table 2.3-1. Characteristics of oil used in the spill simulations.....3
Table 3.2-1. Oil droplet size distribution for the subsea blow-out at the Hebron platform.....13
Table 4.1-1. Summary of the stochastic simulations of the platform and subsea blow-outs at the Hebron well site. The 50th and 95th percentile values are determined by ranking all 100 spills in each scenario according to the area of sea surface exposed to oil, the length of shoreline exposed to oil and the volume of entrained (naturally dispersed) oil above the stated thresholds. 15
Table 4.1-2. Summary of stochastic simulations of the batch transfer spills modeled at the Hebron well site. The 95th percentile values are determined by ranking all 100 spills in each scenario according to the area of sea surface exposed to oil, the length of shoreline exposed to oil and the volume of entrained (naturally dispersed) oil above the stated thresholds. 16
Table 4.2-1. Summary of the deterministic model results. The percentages in the table are the fraction of oil volume in each location or weathering category at the end of the simulation. 18
Table 4.3-1. Newfoundland shoreline oiling summary. Values listed are from the individual spill within each stochastic scenario that resulted in the largest volume of oil stranded on the shore. 19
Table A-1. Definition of four distillation cuts and the eight pseudo-components in the model (monoaromatic hydrocarbons, MAHs; benzene + toluene + ethybenzene + xylene, BTEX; polynuclear aromatic hydrocarbons, PAHs).....3
Table A2: Summary of oil-in-ice advection and weathering effects accounted for in the SIMAP model. 4

1. Introduction

ExxonMobil Canada Properties (EMCP) has contracted ASA for oil spill modeling services to simulate spills at locations off the coast of Newfoundland. The SIMAP model was used to simulate spills of fuel oil in Bull Arm, Trinity Bay, and crude and fuel oil spills at the Hebron offshore site southeast of St. John's. The model scenarios use wind data obtained from model hindcasts and field measurements, and current data from multiple hydrodynamic models. The SIMAP model was used in stochastic and deterministic modes to determine the range of possible water surface oiling, oil in the water column and shoreline oiling predicted to occur.

This report presents the model input data, describes the models applied to simulate the hydrodynamics and the oil spills, and presents and discusses the results of simulations performed at the Hebron well site. A companion report provides the same information for spill simulations performed at the Nalcor Energy Bull Arm Fabrication Site (Bull Arm Site).

2. Model Inputs and Spill Scenarios

The spill scenarios modeled were defined in consultation with EMCP and ExxonMobil Biomedical Sciences to represent the spills that may occur at the offshore Hebron production site. Possible spills at the offshore site include crude oil from a well blow-out, either at the seabed or from the top of the drilling platform, and small volume batch spills of crude and diesel fuel on the sea surface.

Two model systems were used to simulate the spills. The ASA blow-out model simulates the near-field dynamics of the plume of gas/oil mixture discharged from the subsea well blow-out, and the SIMAP model simulates the far-field transport and weathering of the oil released into the water column or at the surface. This section describes the spill scenarios used and the wind, current and ice data defining the environment.

2.1 Study Area

The Island of Newfoundland located in the North Atlantic off the east coast of Canada. The relatively shallow waters of the Continental Shelf extend eastward up to 500 km from the Newfoundland coast. Known as the Grand Banks, this area contains significant petroleum resources. The Hebron well is located near the edge of the Grand Banks, more than 300 km east of St John's (Figure 2.1-1). Bull Arm is a small, relatively deep fjord at the southwest corner of Trinity Bay.

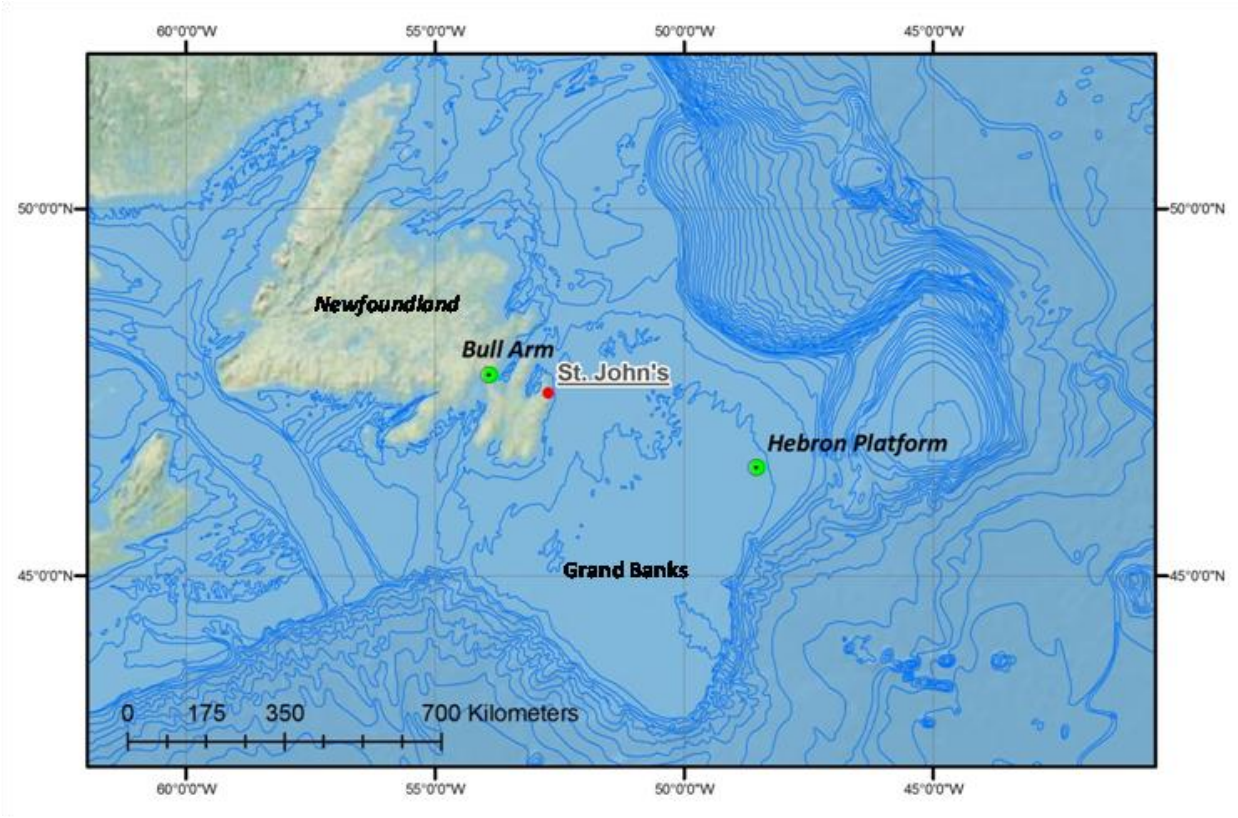


Figure 2.1-1. Map showing the Newfoundland region.

2.2 Model Scenarios

Multiple spill scenarios were modeled to assess the fate of oil spilled from the offshore Hebron well location. All spill scenarios are simulated without any spill countermeasures applied. Two kinds of blow-outs were simulated at the Hebron well site. One blow-out originates at the platform 70 m above the sea surface. The other blow-out originates at a wellhead on the seabed in approximately 98 m water depth.

The platform blow-out introduces Hebron D-94 crude oil onto the sea surface during a long-term, continuous release. This spill is simulated using the SIMAP 3D fates model. To reproduce the dynamic and complex processes of a subsea blow-out, a near-field analysis using ASA's blow-out plume model was performed prior to simulating the far-field movement of the oil in SIMAP.

A series of 6 small volume batch spills were also modeled at the Hebron site. The batch spills include diesel fuel released instantaneously onto the sea surface and crude oil spills released onto the sea surface over a 24-hour period.

Table 2.2-1 lists the specifics for the spill scenarios. The characteristics of the spilled oils are discussed in more detail in Section 2.3.

TABLE 2.2-1. OIL SPILL SCENARIOS MODELED AT THE HEBRON PLATFORM LOCATION.

Scenario	Total Spill Volume	Spill Duration	Season
Offshore - Hebron Platform Site (46.5440573° N, 48.49803617° W)			
Platform Blow-out (D-94 crude) (5,600 m^3/day (35,000 bpd))	166,936.6 m^3 (1,050,000 bbl)	30 days	Summer
	166,936.6 m^3 (1,050,000 bbl)	30 days	Winter
	166,936.6 m^3 (1,050,000 bbl)	30 days	Winter (ice present)
	556,455.4 m^3 (3,500,000 bbl)	100 days	Summer
	667,746.5 m^3 (4,200,000 bbl)	120 days	Winter
	667,746.5 m^3 (4,200,000 bbl)	120 days	Winter (ice present)
Offshore - Hebron Subsea Site (46.5754111° N, 48.3956028° W)			
Subsea Blow-out (Ben Nevis crude) (3,200 m^3/day (20,000 bpd))	317,975 m^3 (2,000,000 bbl)	100 days	Summer
	381,569 m^3 (2,400,000 bbl)	120 days	Winter
	381,569 m^3 92,400,000 bbl)	120 days	Winter (ice present)
Offshore Batch Spill Site (46.5440573° N, 48.49803617° W)			
Batch Transfer (marine diesel)	800 m^3 (5,031 bbl)	Instantaneous	Summer
	800 m^3 (5,031 bbl)	Instantaneous	Winter
	800 m^3 95,031 bbl)	Instantaneous	Winter (ice present)
Batch OLS Transfer (crude oil)	5,000 m^3 (31,449 bbl)	24 hours	Summer
	5,000 m^3 (31,449 bbl)	24 hours	Winter
	5,000 m^3 (31,449 bbl)	24 hours	Winter (ice present)

Note that the 30-day duration blow-out scenarios were also run using a 60-day duration in order to track the oil for an additional 30 days. These extended simulations use the same blow-out duration, rate of release and total release volume as the 30 days scenarios; however, the model run time is extended to 60 days.

2.3 Oil Characterization

The characteristics of the oil types used in the spill simulations are listed in table 2.3-1.

TABLE 2.3-1. CHARACTERISTICS OF OIL USED IN THE SPILL SIMULATIONS.

Oil	Spill	API Gravity	Density (g/cm^3)	Viscosity (cP)
Hebron D-94 Crude	Platform blow-out Batch OLS Transfer	20.1	0.92691 @ 25° C	265.374 @ 25° C
Ben Nevis L55 Well	Subsea blow-out	30.8	0.8711 @ 15° C	15.556 @ 25° C
Marine Diesel Fuel	Batch Transfer Spills	37.6	0.82910 @ 25° C	4.0 @ 25° C

2.4 Wind Data

Wind data for offshore model simulations were obtained from two sources. One source is the MSC50 Wind Hindcast (Swail et al., 2006), a model reanalysis product that provides hindcast winds for the North Atlantic for the period 1954 through 2008. The data are supplied at evenly spaced points 0.1° apart by Environment Canada, MSC Atlantic Operations. Additional wind data were obtained from the National Centers for Environmental Prediction (NCEP) at multiple locations across the North Atlantic. Figure 2.4-1 is a map showing the locations of the MSC50 (sites clustered around the Hebron well site) and NCEP (more widely spaced points in the North Atlantic) wind data locations. Oil spill simulations were run using summer and winter season winds in order to capture these seasonal differences.

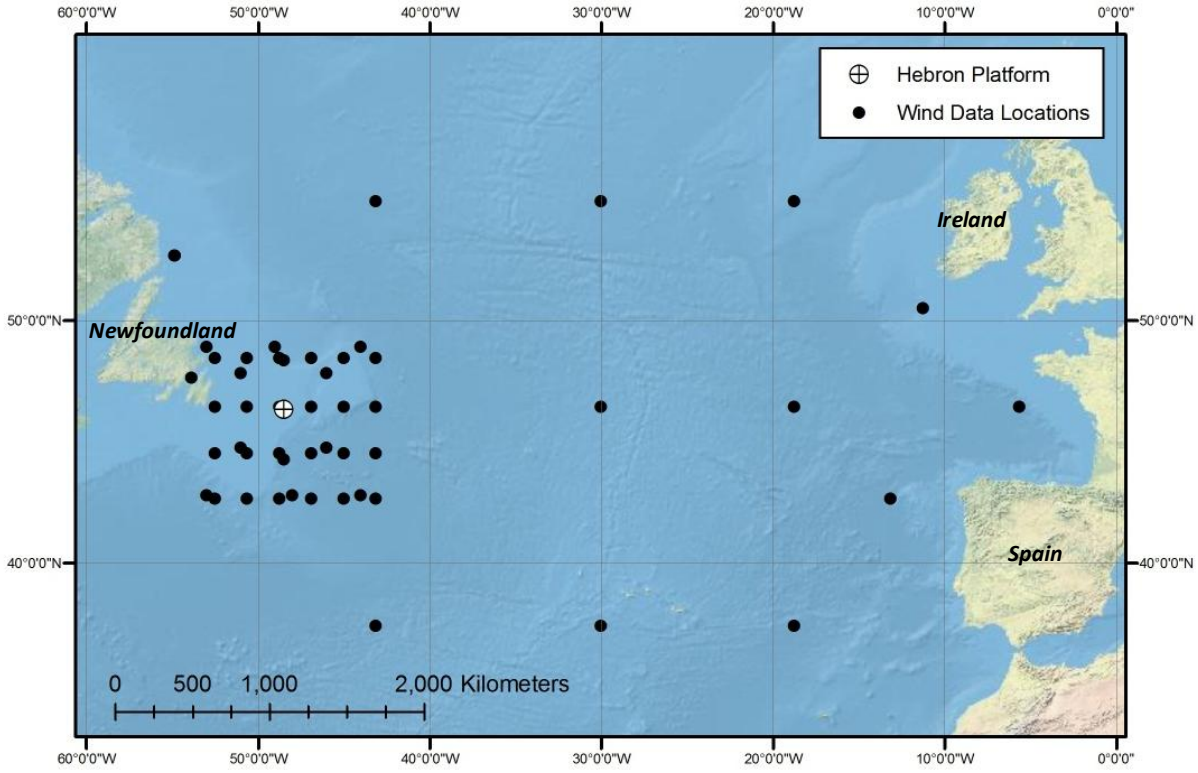


Figure 2.4-1. Map showing the locations of wind data stations for the offshore modeling.

Figure 2.4-2 is a wind rose showing the distribution of annual wind directions and speeds from the MSC50 model hindcast data obtained for location M6010632 adjacent to the offshore well site. The wind comes from all directions at this site, but it comes most frequently from the northwest through the south. There is seasonality in the wind at this location that differentiates the summer and winter seasons. Figure 2.4-3 is the wind rose from the M6010632 location for the winter months. Figure 2.4-4 is the wind rose from the same MSC50 data location for the summer months. Winter wind speeds are higher than in summer and more frequently from the west and north.

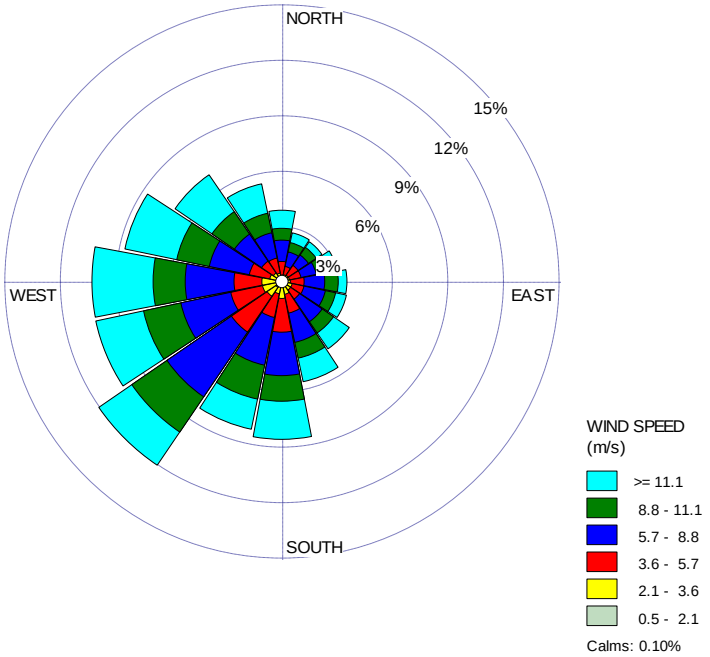


Figure 2.4-2. Wind rose of the MSC50 wind data from site M6010632 near the Hebron platform location for all months of the year. The plot indicates the direction from which the wind is coming for the 30 years 1976 through 2008.

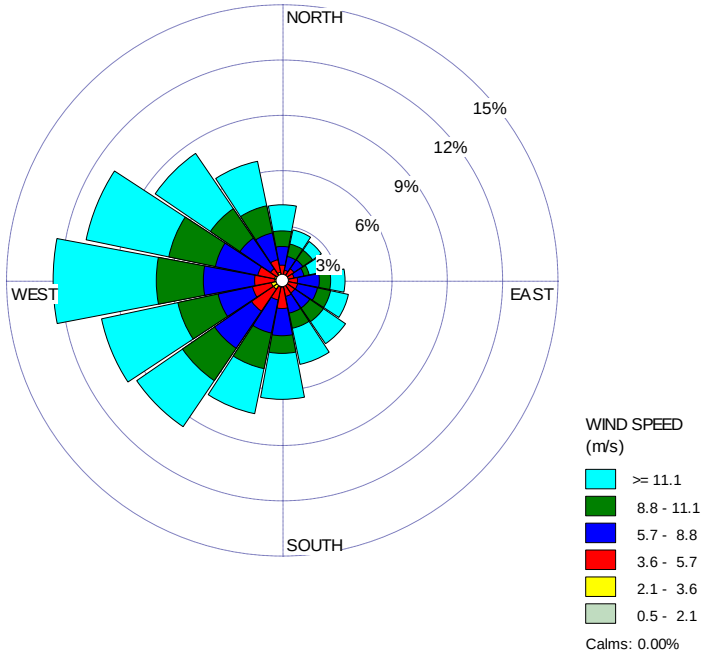


Figure 2.4-3. Wind rose of the MSC50 wind data from site M6010632 near the Hebron platform location for winter months. The plot indicates the direction from which the wind is coming for the 30 years 1976 through 2008.

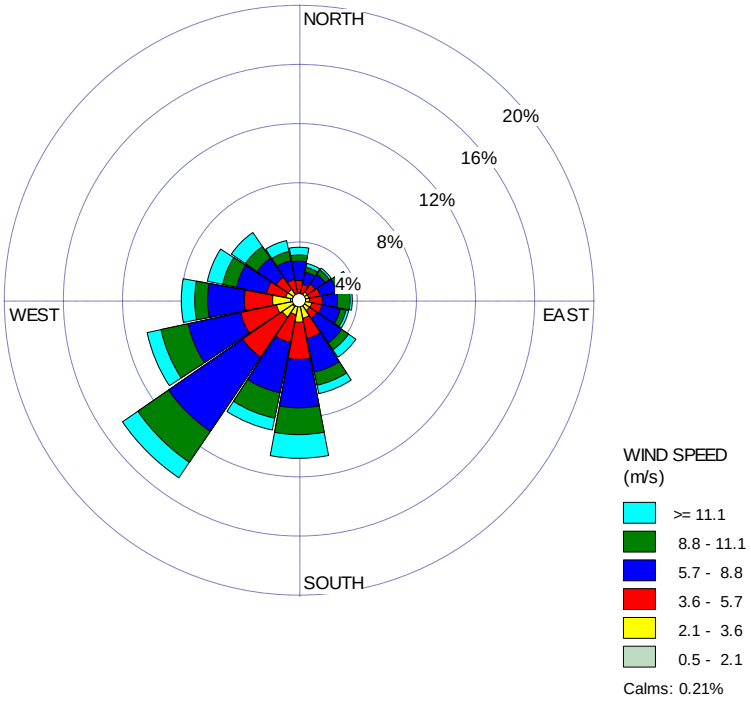


Figure 2.4-4. Wind rose of the MSC50 wind data from site M6010632 near the Hebron platform location for summer months. The plot indicates the direction from which the wind is coming for the 30 years 1976 through 2008.

2.5 Current Data

The Labrador Current dominates the large-scale ocean circulation in the Newfoundland region. This current originates in the Arctic Ocean and flows south along the coasts of Labrador and Newfoundland (see Figure 2.5-1). Currents at smaller scales can be highly variable and it was necessary to develop hydrodynamic model datasets to describe the currents at the offshore site sufficient to simulate the movement of spilled oil.

For this study, currents for the North Atlantic region were acquired from the HYCOM (HYbrid Coordinate Ocean Model) circulation model. HYCOM is a primitive equation ocean general circulation model that evolved from the Miami Isopycnic-Coordinate Ocean Model (MICOM) (Halliwell et al., 1998, 2000; Bleck, 2002). MICOM has become one of the premier ocean circulation models, having been subjected to validation studies (Chassignet et al., 1996; Roberts et al., 1996; Marsh et al., 1996) and used in numerous ocean climate studies (New and Bleck, 1995; New et al., 1995; Hu, 1996, 1997; Halliwell, 1997, 1998; Bleck 1998). Further details on HYCOM can be found on the HYCOM consortium website (http://www.hycom.org).

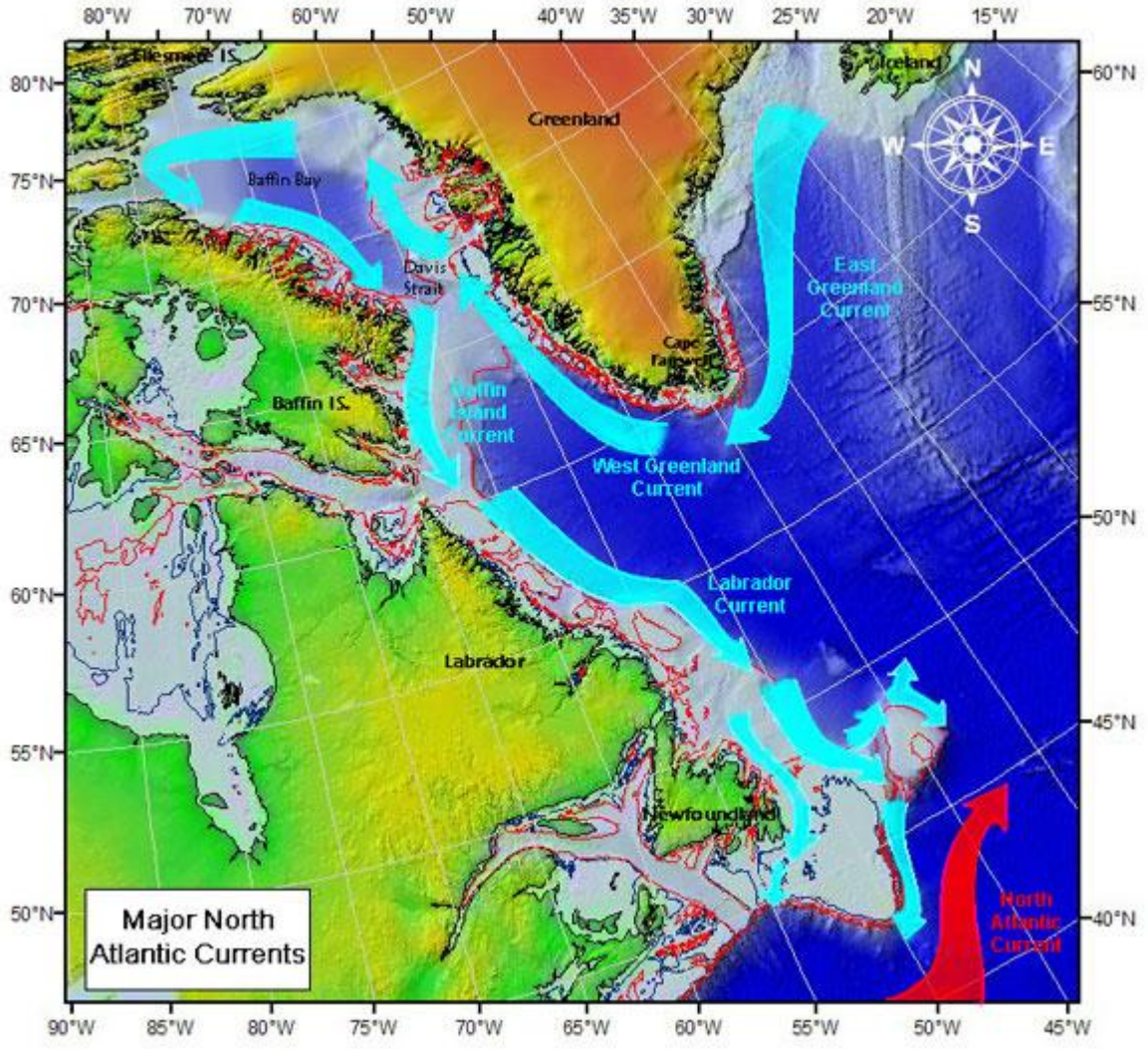


Figure 2.5-1. Map of the large scale ocean currents in the Newfoundland region. (Source: U.S. Coast Guard, International Ice Patrol).

Hindcast currents from the HYCOM model were obtained for the period November 2003 through September 2010 for the North Atlantic region. The current speed and direction data are provided at locations on a regular grid spaced at a distance of 1/12 degree. These currents were used in SIMAP for modeling oil spills originating at the Hebron platform and from the subsea blow-out.

2.6 Ice Data

Sea ice is formed in the autumn in the Arctic and sub-Arctic regions of the world. The growth rate of sea ice depends on surface temperature, the depth of snow cover, and the heat flux in the underlying water. The formation and development of sea ice follows a progression of stages.

The exact timing of these stages at any location is not the same from year to year because of subtle differences in climatic conditions. In the Northern Hemisphere during September and October, the air temperature lowers sufficiently to form a thin sheet of ice on the sea. Freezing temperature for average northern ocean salt water of about 3.5 percent salt composition by weight (usually designated 35 parts per thousand) is -1.8°C (28.8°F).

The presence of sea ice in Newfoundland and Labrador waters was below normal during the winter of 2009-2010 (CIS, 2010). The total accumulated ice coverage in east Newfoundland waters set a new record low during last year's winter season. Figure 2.6-1 shows the total accumulated ice coverage offshore the Canadian east coast measured by the Canadian Ice Service since the winter of 1968-69. With the exception of the 2002-2003 ice season, ice coverage over the past 15 years has been below the 40-year average.

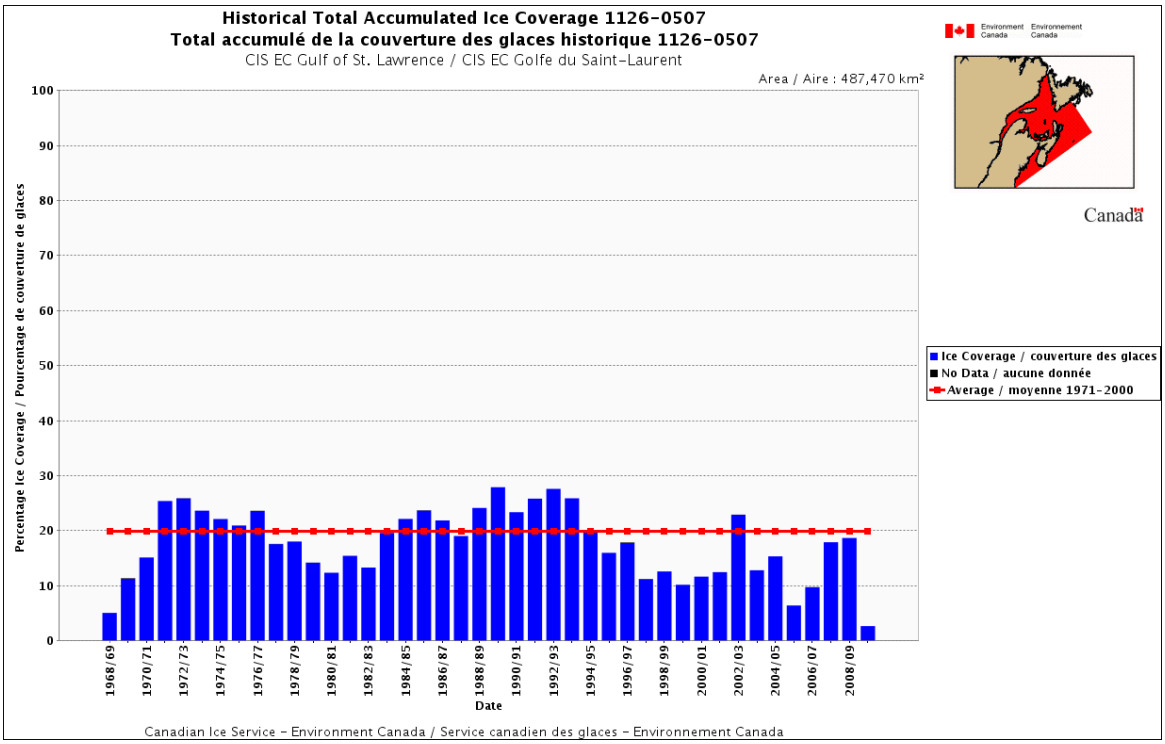


Figure 2.6-1. Total accumulated ice coverage for the period of record from the Canadian Ice Service.

Ice coverage in the winter of 1989-1990 was at a maximum extent according to the data collected by the Canadian Ice Service. Figure 2.6-2 shows a map of ice concentration in the Newfoundland region for the week of March 12, 1990. The red areas on the map in Figure 2.6-2 show that 100% ice concentration covers portions of the offshore area east of Newfoundland. The Hebron platform is located at 48.498° W, 46.544° N.

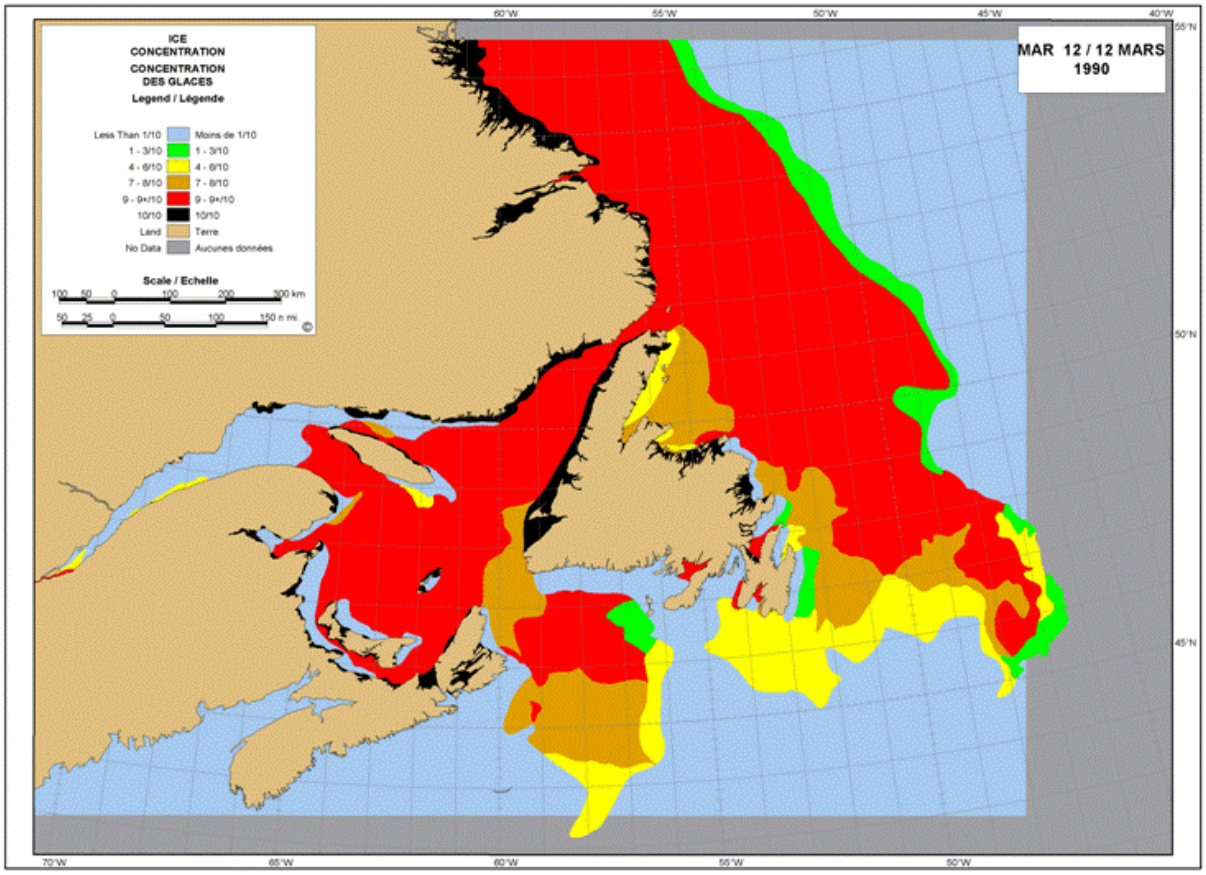


Figure 2.6-2. Ice concentration chart form the Canadian Ice Service for the week of 12 March, 1990.

The fate and behavior of spilled oil is greatly affected by the presence of ice. Oil spilled before, during or after freeze-up will follow an arrested pattern of weathering compared to oil spilled on open water. Implementation of algorithms for modeling the movement and fate of oil in the presence of sea ice is based on the percent of ice coverage. From 0 to 30% coverage, the ice has no effect on the advection or weathering of a surface oil slick. From 30 to 80% ice coverage, oil advection is steered to the right in the northern hemisphere, surface oil thickness generally increases due to ice-restricted spreading, and evaporation and entrainment are both reduced. Above 80% ice coverage, surface oil moves with the ice, evaporation and entrainment cease and oil thickness, which can vary widely, is calculated as a function of ice thickness. Appendix A contains a brief summary of the algorithms implemented in the SIMAP model for oil spills in sea ice conditions.

Ice data used in the oil spill model simulations were obtained from the National Snow and Ice Data Center (http://nsidc.org/index.html) for the months of February and March, 1990. Since 1990 showed the greatest extent of ice coverage, this year was selected as the representative year for the purposes of spill trajectory modeling. These data are in the form of ice

concentration grids with values from 0 to 100% ice coverage. The winter blow-out scenarios run with ice present use these data to define the ice coverage for the months of February and March, regardless of the year. Figure 2.6-3 shows the ice concentration for February, Figure 2.6-4 is a map of the ice concentration for March.

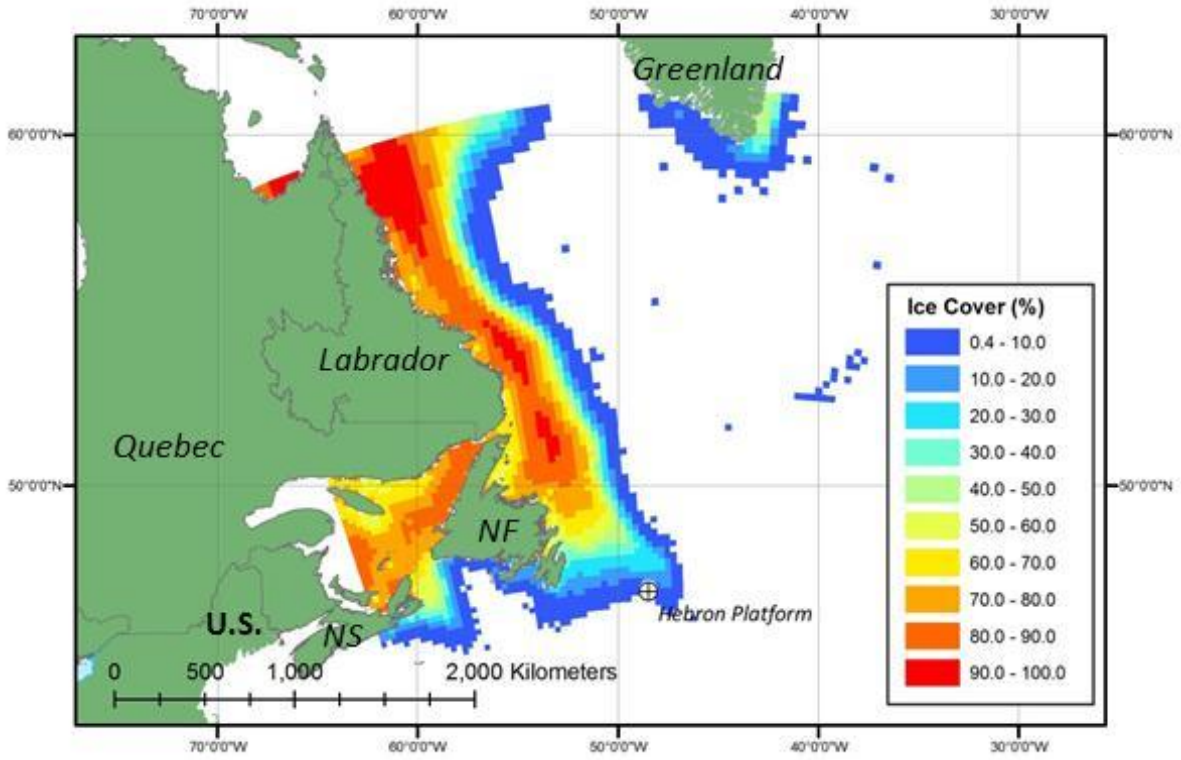


Figure 2.6-3. Sea ice coverage used in the oil spill model simulations for the month of February.

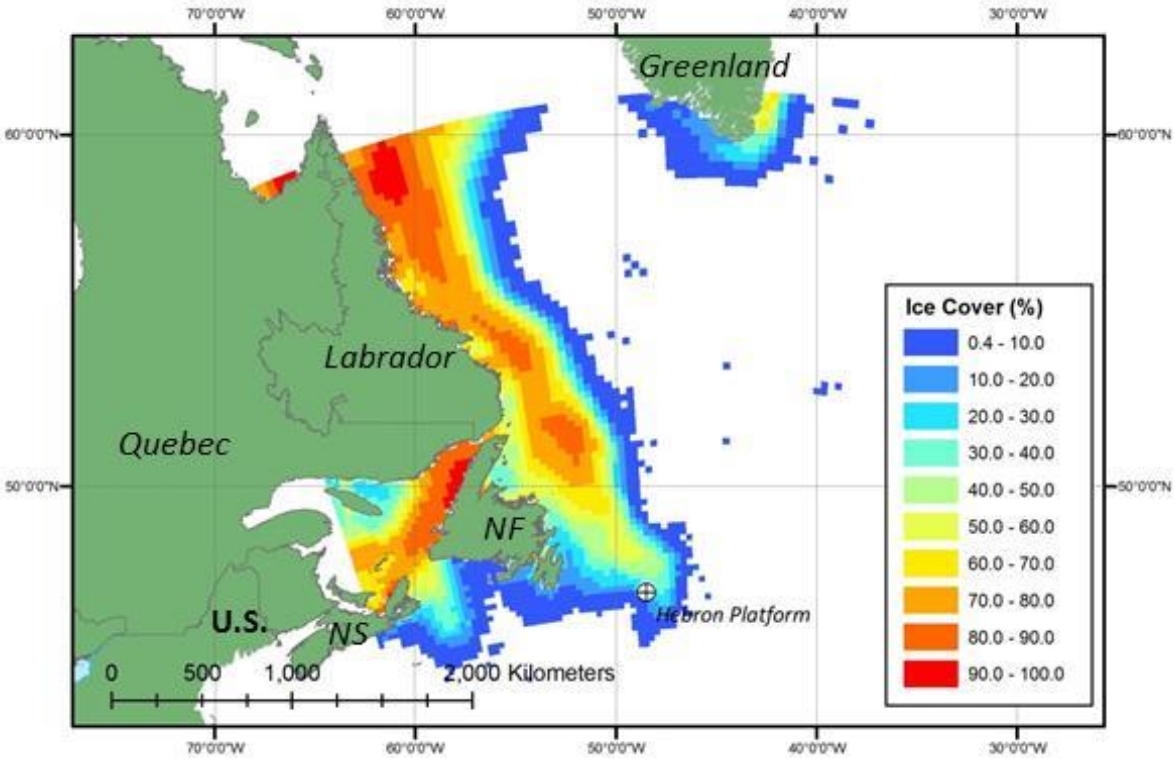


Figure 2.6-4. Sea ice coverage used in the oil spill model simulations for the month of March.

3. Modeling Description

3.1 Blow-outs of Crude Oil

Blow-outs

Two blow-out scenarios were simulated at the Hebron offshore site. A blow-out is defined as the uncontrolled release of hydrocarbons from the wellbore. One discharge originates from the platform deck at a height of 70 m above the sea surface; the subsea blow-out occurs at the seabed in 98 m of water. The SIMAP stochastic and deterministic models were used to simulate the crude oil releases. The subsea blow-out is modeled using the ASA blow-out model in combination with the SIMAP stochastic and 3D fates models. The blow-out originating from the platform is simulated as a surface release using the SIMAP stochastic and 3D fates models.

ASA's blow-out model was used to determine the near-field dynamics of the oil plume for the release occurring at the seabed. When blow-outs occur in deep water, it is necessary to use a model that considers the effects of gas hydrate formation and calculates the size of oil droplets discharged from the source in order to determine the movement of oil through the water column to the sea surface. In this case, the 98 m water depth at the Hebron offshore site is too shallow for hydrate formation, so that process is not included in this modeling study.

ASA's blow-out plume model predicts the dynamics of deep-water blow-outs by solving equations for the conservation of water mass, momentum, buoyancy, and oil/gas mass using integral plume theory, following McDougall (1978). Equilibrium hydrate formation and dissociation for gas hydrates are determined by a multi-phase flash calculation developed by Bishnoi et al. (1979, 1989). Appendix B describes the blow-out plume model. Results from the blow-out plume modeling provide the initial dynamics of the oil plume for the 3D fates simulations (i.e., far-field analysis) of the subsea blow-out.

In a blow-out, an oil and gas mixture is released from the seabed and is driven into the water column, where it initially forms a momentum jet. Depending on the velocity of the gas/oil mixture exiting the well, the jet portion of the discharge can be confined to the vicinity of the seabed or extend vertically into the water column for hundreds of meters. As the jet-driven plume rises, it continues to entrain sea water, reducing the plume's velocity and buoyancy and increasing its radius, forming the shape of an inverted cone. Figure 3.2-1 shows a perspective view of an idealized terminated plume for a simple case with no currents to distort the plume. At the point above the seabed where the jet is no longer driven by the discharge momentum and buoyancy of the gas, the oil droplets are driven towards the sea surface by buoyant force. If the momentum-driven jet reaches the sea surface, the plume is deflected in a radial, surface flow zone without appreciable loss of momentum. This radial jet carries the oil particles rapidly away from the center of the plume. The velocity and oil concentrations in this surface flow zone decrease while the depth of the zone increases. In the far-field, where the plume buoyancy has been dissipated, ambient currents and wind generated waves determine the subsequent transport and dispersion of the oil.

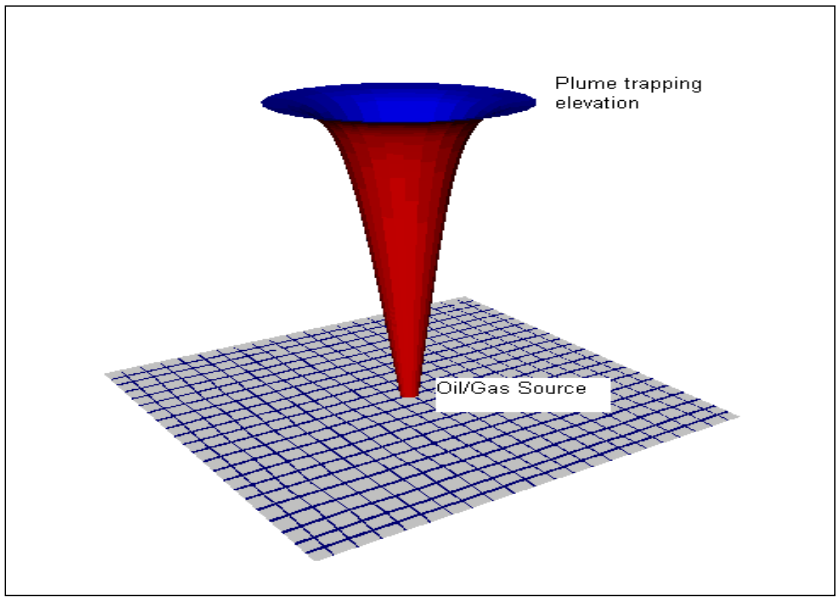


Figure 3.2-1. Perspective view of example oil/gas plume reaching termination depth.

Blow-out Plume Dynamics

Oil ascends to the surface essentially with the same path as the gas. The oil initially rides on the buoyant plume; after leaving the plume, it rises with the free-rise velocities determined by Stokes law. The free-rise velocities of oil are significantly slower than that of gas due to the lower density difference (water/oil) and a much smaller range of oil droplet sizes.

The size range of the oil droplets produced during the blow-out has a profound effect on how oil travels after leaving the plume. Large droplets will reach the surface faster and small droplets will stay longer in the water column and be subjected to the subsea advection-diffusion transport from ocean currents and turbulence for a longer period. Long residence time in the water column means that oil droplets have the potential to be transported long distances from the blown out well before reaching the sea surface.

The oil droplet size distribution used in the blow-out model is based on the Rosin-Rammler distribution (Rye et al., 1998, Lefebvre, 1989), and primarily depends on the exit velocity of the discharged oil and gas. For a given exit dimension, exit velocity is a function of total discharge rate. Table 3.2-1 lists the droplet size distribution used to simulate the subsea blow-out. Once a size distribution is determined, rise velocities are a function of droplet size. The oil droplet size distributions in Table 3-2.1, as well as the width and height of the plume determined using the blow-out model, were used in the SIMAP 3D fates model to initialize the subsea blow-out simulations. The blow-out model predicts that the oil will be delivered to the top 10 m of the water column as oil droplets with the size distribution listed in Table 3.2-1.

TABLE 3.2-1. OIL DROPLET SIZE DISTRIBUTION FOR THE SUBSEA BLOW-OUT AT THE HEBRON PLATFORM.

Droplet Size (microns)	Volume %
64.5	16.5
129.0	26.0
193.5	23.6
258.0	17.2
322.5	10.8
387.0	6.0

The blow-out originating on the Hebron platform 70 m above the sea surface does not require the use of the blow-out model. This release was simulated using the SIMAP 3D fates model as a surface blow-out. The gas/oil mixture exiting the well pipe will form a jet extending tens of meters into the air before the oil that is discharged settles on the water surface in a circular area surrounding the platform, defined in the model as a circle of 200 m in diameter.

3.2 Batch Transfer Spills

Small volume crude oil and marine diesel spills were simulated at the Hebron platform site. Both of these spills are short-term releases at the sea surface (see Table 2.2-1 for spill volumes and durations).

4. Model Results

The stochastic and deterministic model results are presented and discussed in Section 4. Maps of the stochastic modeling results are presented in Appendix C, followed by results from the 3D fates deterministic modeling in Appendix D.

4.1 Stochastic Model Results

The stochastic model is used to determine the probability that oil on the water surface and the shoreline will exceed the thickness threshold of 0.01 mm and that oil dispersed into the water column by natural processes will exceed a concentration threshold of 10 ppb (parts per billion). Maps of the stochastic model results in Appendix C show the predicted probability of oil exceeding the thickness and concentration thresholds as well as the minimum time required for thresholds to be exceeded within the oil probability footprint.

Summary of Stochastic Model Results for Blow-outs

Table 4.1-1 summarizes the results from the stochastic modeling of the platform and subsea blow-outs. The table lists the results from the stochastic model for individual simulations ranked as the 50^{th} and 95^{th} percentile for oiled sea surface area, oiled shoreline length and entrained oil volume.

Note that the 30-day duration blow-out scenarios were also run using a 60-day duration in order to track the oil for an additional 30 days. These extended simulations use the same blow-out duration, rate of release and total release volume as the 30-day scenarios; however, the model run time was extended to 60 days. The purpose of the extended period 30-day spill scenarios is to determine when and where oil contacts the Newfoundland shoreline. A summary of the spills resulting in oil contact with the Newfoundland shoreline are presented in a subsequent subsection later in section 4.1.

Winds and currents at the Hebron well site are such that the majority of spills are predicted to travel eastward. The distance traveled is controlled by the blow-out duration and the strength and consistency of direction of the wind. Winter wind speeds are higher than in summer and more frequently from the west and north, which drives oil greater distances to the east than summer winds. A subset of the summer and winter spill simulations of greater than 30 days duration are predicted to reach segments of the Newfoundland shoreline.

Both of the crude oils used in the simulations are persistent and do not disperse into the water column readily from natural processes. This characteristic, combined with the long duration release of oil into the water, result in a large fraction of the oil remaining on the sea surface. The area of sea surface exposed to floating oil increases linearly with an increase in total spill volume.

TABLE 4.1-1. SUMMARY OF THE STOCHASTIC SIMULATIONS OF THE PLATFORM AND SUBSEA BLOW-OUTS AT THE HEBRON WELL SITE. THE 50TH AND 95TH PERCENTILE VALUES ARE DETERMINED BY RANKING ALL 100 SPILLS IN EACH SCENARIO ACCORDING TO THE AREA OF SEA SURFACE EXPOSED TO OIL, THE LENGTH OF SHORELINE EXPOSED TO OIL AND THE VOLUME OF ENTRAINED (NATURALLY DISPERSED) OIL ABOVE THE STATED THRESHOLDS.

Oil Release	Season	Sea Surface Area Oiled at > 0.01mm (km^2)		Shoreline Length Oiled at > 0.01mm (km)		Entrained Oil Volume after 30 days (m^3)	
		50^{th} Percentile	95^{th} Percentile	50^{th} Percentile	95^{th} Percentile	50^{th} Percentile	95^{th} Percentile
Platform Blow-out	Summer 30-Day	205,661	388,892	0	0	20,717	31,200
	Winter 30-Day	416,325	586,907	0	0	27,428	71,582
	Winter 30-Day Ice	446,821	646,973	0	0	27,478	55,122
	Summer 30-/60-Day	963,319	1,383,242	0	0	434	501
	Winter 30-/60-Day	1,462,785	1,901,033	0	47.7	480	573
	Winter 30-/60-Day Ice	1,382,033	1,791,808	0	42.4	476	550
	Summer 100-Day	1,855,219	2,306,565	0	10.6	134,106	159,925
	Winter 120-Day	3,353,447	4,225,306	63.6	636.2	198,454	263,493
	Winter 120-Day Ice	3,981,644	4,841,586	148.4	742.2	198,454	263,493
Subsea Blow-out	Summer 100-Day	1,942,295	2,416,717	0	5.3	3,403,664	3,706,057
	Winter 120-Day	3,535,976	4,415,367	42.4	466.5	3,777,843	4,309,446
	Winter 120-Day Ice	3,741,889	4,615,041	53	471.8	3,814,887	4,182,299

Summary of Stochastic Model Results for Batch Transfer Spills

Table 4.1-2 summarizes the results from the stochastic modeling of the batch transfer spills performed at the Hebron well site location. The table lists the results from the stochastic model for individual simulations ranked as the 50th and 95th percentile for oiled sea surface area, oiled shoreline length and entrained oil volume. The 95th percentile results correspond to the maps of deterministic model results shown in Appendix D.

TABLE 4.1-2. SUMMARY OF STOCHASTIC SIMULATIONS OF THE BATCH TRANSFER SPILLS MODELED AT THE HEBRON WELL SITE. THE 95TH PERCENTILE VALUES ARE DETERMINED BY RANKING ALL 100 SPILLS IN EACH SCENARIO ACCORDING TO THE AREA OF SEA SURFACE EXPOSED TO OIL, THE LENGTH OF SHORELINE EXPOSED TO OIL AND THE VOLUME OF ENTRAINED (NATURALLY DISPERSED) OIL ABOVE THE STATED THRESHOLDS.

Oil Release	Season	Surface Area Oiled at > 0.01mm (km^2)	Shoreline Oiled at > 0.01mm (km)	Entrained Oil Volume after 30 days (m^3)
		95th Percentile	95th Percentile	95th Percentile
Batch Transfer	Summer	251,672	0	496
	Winter	447,298	0	548
	Winter w/ Ice	461,520	0	547
Batch OLS Transfer	Summer	250,351	0	25
	Winter	433,132	0	28
	Winter w/ Ice	454,550	0	32

Similar to the blow-outs of crude oil reported above, marine diesel and crude oil released in the batch transfer spills is predicted to travel primarily toward the east away from the Island of Newfoundland. The marine diesel fuel is more easily dispersed into the water column than the crude oil, as can be seen in the quantity of entrained oil in Table 4.1-2. The marine diesel is capable of achieving a smaller minimum thickness than the crude oil, resulting in a relatively higher sea surface area exposed to oil. None of the batch transfer spills are predicted to reach the Newfoundland shoreline.

4.2 Deterministic Model Results

This section presents and discusses the results from the deterministic model simulations of platform and subsea blow-outs and from the batch transfer spills. Maps of the deterministic model output in Appendix D depict the results from one model simulation chosen from the 100 individual simulations completed by the stochastic model. The simulations were selected because they rank as the 95th percentile for sea surface area exposed to oil, shoreline length exposed to oil, or entrained (water column) oil volume exceeding the stated thresholds. It should be kept in mind that each map in Appendix D displays the results from an individual spill simulation.

Platform blow-out scenarios simulated a release of 35,000 bbl of Hebron D94 crude onto the sea surface daily for a period of between 30 and 120 days. Winter and summer environmental conditions were used to determine the seasonal variability in the oil trajectory and weathering.

Subsea blow-outs were simulated by releasing 20,000 bbl of Ben Nevis crude daily into the water column above the well for a period of 100 and 120 days. Winter season conditions were simulated with and without sea ice present for both the platform and subsea blow-outs. Batch transfer spills include an instantaneous release of 5,031 bbl of marine diesel and 31,449 bbl of D-94 crude oil over 24 hours at the sea surface.

Table 4.2-1 summarizes the results from the deterministic model runs.

Platform Blow-out

The volume of oil remaining on the sea surface at the end of each model simulation ranges from 51% to 79% of the total volume released. In general, as the oil release duration increases, the fraction of oil remaining on the sea surface decreases. This relative decrease in surface oil corresponds with an increase in the rate of natural decay. Decay, which accounts for 12% to 37% of the total platform blow-out spill volume, occurs as the result of photolysis, a chemical process energized by ultraviolet light from the sun, and by biological breakdown from organisms in the water. The decrease in surface oil over time may in some instances correspond to surface oil stranding on the shoreline, reducing the amount of oil on the surface.

While the fraction of surface oil volume is predicted to decrease over time, the sea surface area covered by oil thicker than 0.01 mm is predicted to increase as the duration of the blow-out increases. The increase in sea surface area exposed to oil is due to the rapid and continual spreading of the surface slick.

The fraction of oil lost to evaporation does not vary greatly, ranging from 7.8% to 11.4% of the total volume released. The amount of oil entrained in the water column through natural dispersion processes is less than 0.5% for all platform blow-out spill scenarios.

Subsea Blow-out

The volume of oil remaining on the sea surface at the end of each of the subsea blow-out simulations ranges from 29% to 35%, considerably less than the platform blow-outs. The subsea blow-out introduces oil directly into the water column, where it makes up 9% to 10% of the spilled volume throughout the duration of the blow-out. As with the platform blow-out, as the oil release duration increases, the fraction of oil remaining on the sea surface decreases due to an increasing rate of natural decay. Decay accounts for 26% to 30% of the released oil.

Oil lost to evaporation in the subsea blow-out spills is predicted to be more than twice the amount in the platform blow-outs, ranging from approximately 29% to 32%. This is due primarily to differences in the physical and chemical makeup of the Ben Nevis crude compared to the Hebron D94 crude oil.

TABLE 4.2-1. SUMMARY OF THE DETERMINISTIC MODEL RESULTS. THE PERCENTAGES IN THE TABLE ARE THE FRACTION OF OIL VOLUME IN EACH LOCATION OR WEATHERING CATEGORY AT THE END OF THE SIMULATION.

Release Type	Spill Scenario	Total Spill Volume (m^3)	Surface Oil (%)	Evap. (%)	Water Column (%)	Oil Ashore (%)	Oil Decayed (%)
Platform Blow-out	Summer 30-day	168,000	79	8.2	0.2	0	12.6
	Winter 30-day	168,000	79	8.3	0.2	0	12.5
	Winter – ice 30-day	168,000	79	7.8	0.2	0	13
	Summer 30-/60-day	168,000	56	11.7	0.3	0	32.0
	Winter 30-/60-day	168,000	56	11.3	0.3	0.2	32.2
	Winter – ice 30-/60-day	168,000	56	11.3	0.3	0.01	32.4
	Summer 100-day	560,000	56	10.2	0.2	0.02	33.6
	Winter 120-day	672,000	51	11.4	0.3	0.4	36.9
	Winter – Ice 120-day	672,000	51	11.2	0.3	0.4	37.1
Subsea Blow-out	Summer	320,000	35	28.6	9.9	0	26.5
	Winter	384,000	31	29.8	9	0.09	30.1
	Winter - ice	384,000	29	32.3	9.1	0.2	29.4
Batch Transfer	Summer	800	0	45.2	39.6	0	15.2
	Winter	800	0	6.4	69.7	0	23.9
	Winter - ice	800	0	6.2	69.8	0	24.0
Batch OLS Transfer	Summer	5,000	64	12.9	0.5	0	22.6
	Winter	5,000	64	12.5	0.5	0	23.0
	Winter - Ice	5,000	64	12.6	0.4	0	23.0

Batch Transfer Spills

None of the marine diesel oil released in the batch transfer spill remains on the sea surface at the end of the 30-day simulation. This is primarily because the diesel is more readily entrained into the water column than the crude oil and in the summer season has a higher rate of evaporation. Between 40 and 70% of the diesel is predicted to become entrained in the water column while 0.4% to 0.5% of the crude will entrain. The model predicts between 15% and 24% of the diesel and 22% to 23% of the crude will decay.

4.3 Newfoundland Shoreline Oiling

Not all of the stochastic model simulations of the platform and subsea blow-outs predict oil will hit the Newfoundland coast. The stochastic model simulations predict a 1% to 6% probability that oil from either the platform or the subsea blow-outs will reach the Newfoundland shore. Spill scenarios where oil is predicted to reach the Newfoundland shoreline are listed in Table 4.3-1. The values listed in the table are from the individual spill from each stochastic model scenario that resulted in the maximum amount of oil on the Newfoundland shore. A zero probability of oiling means that none of the 100 spills completed in the stochastic model scenario reached the Newfoundland coastline.

TABLE 4.3-1. NEWFOUNDLAND SHORELINE OILING SUMMARY. VALUES LISTED ARE FROM THE INDIVIDUAL SPILL WITHIN EACH STOCHASTIC SCENARIO THAT RESULTED IN THE LARGEST VOLUME OF OIL STRANDED ON THE SHORE.

Scenario	Probability of Oiling (%)	First Arrival of Oil (days)	Shoreline Length Oiled (km)	Shoreline Area Oiled (m^2)	Expected Mean Mass (g/m^2)
Surface 30-day Summer	0	-	-	-	-
Surface 30-day Winter	0	-	-	-	-
Surface 30-day Extended Run Summer	0	-	-	-	-
Surface 30-day Extended Run Winter	1	41	142.7	428,100	20
Surface 30-day Extended Run Winter w/ice	0	-	-	-	-
Surface 100-day Summer	1	23	5.3	15,900	0.2
Surface 120-day Winter	1	108	285.5	856,500	20
Surface 120-day Winter w/ice	3	21	137.8	413,500	60
Subsea 100-day Summer	1	39	5.3	15,900	0.8
Subsea 120-day Winter	3	21	127.2	381,600	39
Subsea 120-day Winter w/ice	1	40	116.6	349,900	20
Batch Transfer Summer	0	-	-	-	-
Batch Transfer Winter	0	-	-	-	-
Batch Transfer Winter – w/ice	0	-	-	-	-
Batch OLS Transfer Summer	0	-	-	-	-
Batch OLS Transfer Winter	0	-	-	-	-
Batch OLS Transfer Winter – w/ice	0	-	-	-	-

6. References

ASCE Task Committee on Modeling Oil Spills, 1996. State-of-the-art Review of Modeling Transport and Fate of Oil Spills, Water Resources Engineering Division, ASCE, Journal of Hydraulic Engineering 122(11): 594-609.

Becker,J., D. T. Sandwell, 2008, “SRTM30_PLUS: Data fusion of SRTM land topography with measured and estimated seafloor topography”,SRTM30_PLUS V4.0 May 20, 2008

Boyer, T., S. Levitus, H. Garcia, R. A. Locarnini, C. Stephens, and J. Antonov, 2004 Objective Analyses of Annual, Seasonal, and Monthly Temperature and Salinity for the World Ocean on a ¼ E Grid, Submitted to International Journal of Climatology April 16, 2004, Ocean Climate Laboratory, National Oceanographic Data Center, Silver Spring, Maryland

Bishnoi, P. R. and Mainik B. B., 1979. Laboratory study of behaviour of oil and gas particles in salt water, relating to deepwater blow-outs, Spill Technology Newsletter, Vol. 4 (1), pp. 24-36.

Bishnoi, P. R., Gupta, A. K., Englezos, P., Kalogerakis, N., 1989. Fluid Phase Equilibria, 83, 97.

Bleck, R., 1998: Ocean modeling in isopycnic coordinates. Chapter 18 in Ocean Modeling and Parameterization, E. P. Chassignet and J. Verron, Eds., NATO Science Series C: Mathematical and Physical Sciences, Vol. 516, Kluwer Academic Publishers, 4223-448.

Bleck, R., 2002: An oceanic general circulation model framed in hybrid isopycnic-Cartesian coordinates. *Ocean Modeling*, 4, 55-88.

Boyer, T., S. Levitus, H. Garcia, R. A. Locarnini, C. Stephens, and J. Antonov, 2004 Objective Analyses of Annual, Seasonal, and Monthly Temperature and Salinity for the World Ocean on a ¼ E Grid, Submitted to International Journal of Climatology April 16, 2004, Ocean Climate Laboratory, National Oceanographic Data Center, Silver Spring, Maryland.

Canadian Ice Service, 2010: Seasonal Summary for Eastern Canada, Winter 2009-2010. Produced by the Canadian Ice Service, July, 2010.

Chassignet, E. P., L. T. Smith, R. Bleck, and F. O. Bryan, 1996: A model comparison: numerical simulations of the North and Equatorial Atlantic oceanic circulation in depth and isopycnic coordinates. J. Phys. Oceanogr., 26, 1849-1867.

Egbert, G.D., Bennett, A.F., and M.G.G. Foreman (1994), TOPEX/POSEIDON tides estimated using a global inverse model, J. Geophysical Research, 99, 24821-24852.

Environmental Technology Centre, Environment Canada, 2004. Spills Technology Databases. Oil Properties database. http://www.etc-cte.ec.gc.ca/databases/OilProperties/Default.aspx

French, D., M. Reed, K. Jayko, S. Feng, H. Rines, S. Pavignano, T. Isaji, S. Puckett, A. Keller, F. W. French III, D. Gifford, J. McCue, G. Brown, E. MacDonald, J. Quirk, S. Natzke, R. Bishop, M. Welsh, M. Phillips and B.S. Ingram, 1996a. The CERCLA type A natural resource damage assessment model for coastal and marine environments (NRDAM/CME), Technical Documentation, Vol. I - Model Description. Final Report, submitted to the Office of Environmental Policy and Compliance, U.S. Dept. of the Interior, Washington, DC, April, 1996, Contract No. 14-0001-91-C-11.

French, D., M. Reed, S. Feng and S. Pavignano, 1996b. The CERCLA type A natural resource damage assessment model for coastal and marine environments (NRDAM/CME), Technical Documentation, Vol. III - Chemical and Environmental Databases. Final Report , Submitted to the Office of Environmental Policy and Compliance, U.S. Dept. of the Interior, Washington, DC, April, 1996, Contract No. 14-01-0001-91-C-11.

Gundlach, E.R., 1987. Oil Holding Capacities and Removal Coefficients for Different Shoreline Types to Computer Simulate Spills in Coastal Waters, in Proceedings of the 1987 Oil Spill conference, pp. 451-457.

Halliwell, G. R., Jr., 1997: Simulation of decadal/interdecadal variability the North Atlantic driven by the anomalous wind field. Proceedings, Seventh Conference on Climate Variations, Long Beach, CA, 97-102.

Halliwell, G. R., Jr., 1998: Simulation of North Atlantic decadal/multi-decadal winter SST anomalies driven by basin-scale atmospheric circulation anomalies. Journal of Physical Oceanography, 28, 5-21.

Halliwell, G. R., Jr., R. Bleck, and E. Chassignet, 1998: Atlantic Ocean simulations performed using a new hybrid-coordinate ocean model. EOS, Fall 1998 AGU Meeting.

Halliwell, G .R, R. Bleck, E. P. Chassignet, and L.T. Smith, 2000: mixed layer model validation in Atlantic Ocean simulations using the Hybrid Coordinate Ocean Model (HYCOM). EOS, 80, OS304.

Hu, D., 1996: On the Sensitivity of Thermocline Depth and Meridional Heat Transport to Vertical Diffusivity in OGCMs. J. Physical Oceanography, 26, 1480-1494.

IOC, IHO and BODC (GEBCO) 2003. Centenary Edition of the GEBCO Digital Atlas, published on behalf of the Intergovernmental Oceanographic Commission (IOC) and the International Hydrographic Organization (IHO) as part of the General Bathymetric Chart of the Oceans; British Oceanographic Data Centre (BODC), Liverpool.

Isaji T., E. Howlett, C. Dalton, and E. Anderson, 2001: “Stepwise -Continuous-Variable-Rectangular Grid Hydrodynamics Model”, in Proceedings of the Twenty-fourth Arctic and Marine Oil Spill Program (AMOP) Technical Seminar, Edmonton (Alberta) Canada, pp. 597-610, June 12, 2001

Kullenberg, G. (ed.), 1982. Pollutant transfer and transport in the sea. Volume I. CRC Press, Boca Raton, Florida. 227 p.

Lefebvre, A. H., 1989, Atomization and Sprays, Hemisphere Publishing Corp., New York.

Marsh, R., M. J. Roberts, R. A. Wood, and A. L. New, 1996: An intercomparison of a Bryan-Cox-type ocean model and an isopycnic ocean model, part II: the subtropical gyre and meridional heat transport. J. Phys. Oceanogr., 26, 1528-1551.

McAuliffe, C.D., 1987. Organism exposure to volatile/soluble hydrocarbons from crude oil spills – a field and laboratory comparison. Proceedings of the 1987 Oil Spill Conference, API, p. 275-288.

McDougall, T.J., 1978. Bubble plumes in stratified environments, Journal of Fluid Mechanics, Vol. 85, Part 4, pp. 655-672.

Nafaa, M.G. and O.E. Frihy, 1993. Beach and Nearshore Features Along the Dissipative Coastline of the Nile Delta, Egypt. Journal of Coastal Research, Vol. 9, No. 2 (Spring, 1993), pp. 423-433

National Research Council (NRC), 1985. Oil in the Sea: Inputs, Fates and Effects, National Academy Press, Washington, D.C. 601p.

New, A. and R. Bleck, 1995: An isopycnic model of the North Atlantic, Part II: interdecadal variability of the subtropical gyre. J. Phys. Oceanogr., 25, 2700-2714.

New, A., R. Bleck, Y. Jia, R. Marsh, M. Huddleston, and S. Barnard, 1995: An isopycnic model of the North Atlantic, Part I: model experiments. J. Phys. Oceanogr., 25, 2667-2699.

Okubo, A. 1971. Oceanic diffusion diagrams. Deep-Sea Research 8:789-802.

Okubo, A. and R.V. Ozmidov, 1970. Empirical dependence of the coefficient of horizontal turbulent diffusion in the ocean on the scale of the phenomenon in question atmospheric and ocean physics 6(5):534-536.

Roberts, M. J., R. Marsh, A. L. New, and R. A. Wood, 1996: An intercomparison of a Bryan-Cox-type ocean model and an isopycnic ocean model, part I: the subpolar gyre and highlatitudeprocesses. J. Phys. Oceanogr., 26, 1495-1527.

Rye, H., Johansen, O., and Kolderup, H. 1998. Drop size formation from deep water blow-outs.' *SINTEF Report*

Statoil Memo, " El Dabaa Field – Monthly metocean data", Martin Mathiesen, Polytec Foundation, 9 July 2010.

Swail, V.R., Cardone, V.J., Ferguson, M., Gummer, D.J., Harris, E.L., Orelup, E.A. and A.T. Cox. 2006: The MSC50 Wind and Wave Hindcast Reanalysis, Ninth International Workshop on Wave Hindcasting and Forecasting, September 25-29, 2006. Victoria, B.C., Canada.

VLIZ (2009). Maritime Boundaries Geodatabase, version 5. Available online at http://www.vliz.be/vmdcdata/marbound. Consulted on 2010-10

Appendix A: SIMAP Model Description

SIMAP includes: (1) an oil physical fates model; (2) interfacing to a hydrodynamics model for simulation of currents; (3) a biological effects model; (4) an oil physical, chemical and toxicological database; (5) environmental databases (winds, currents, salinity, temperature); (6) geographical data (in a GIS); (7) a biological database; (8) a response module to analyze effects of response activities; (9) graphical visualization tools for outputs; and (10) exporting tools to produce text format output.

SIMAP originated from the oil fates and biological effects sub-models in the Natural Resource Damage Assessment Model for Coastal and Marine Environments (NRDAM/CME), which ASA developed in the early 1990s for the US Department of the Interior for use in Natural Resource Damage Assessment (NRDA) regulations under the Comprehensive Environmental Response, Compensation and Liability Act of 1980 (CERCLA). The NRDAM/CME (Version 2.4, April 1996) was published as part of the CERCLA type A NRDA Final Rule (Federal Register, May 7, 1996, Vol. 61, No. 89, p. 20559-20614). The technical documentation for the NRDAM/CME is in French et al. (1996a,b,c). This technical development involved several in-depth peer reviews, as described in the Final Rule.

While the NRDAM/CME was developed for simplified natural resource damage assessments of small spills in the United States, SIMAP is designed to evaluate fates and effects of both real and hypothetical spills in marine, estuarine and freshwater environments worldwide. SIMAP may be run in stochastic mode to evaluate a distribution of spill results, rather than just a single result for a specific hind-cast. Additions and modifications to prepare SIMAP were made to increase model resolution, allow modification and site-specificity of input data, allow incorporation of temporally varying current data, evaluate subsea blow-outs and movements of entrained oil, track multiple chemical components of the oil, enable stochastic modeling, and facilitate analysis of results. The consideration of the impacts of entrained oil is important, particularly in the evaluation of impacts on aquatic organisms. Surface floating oil primarily impacts wildlife and intertidal biota, and not aquatic biota in subtidal habitats. At wind speeds higher than about 12 knots (or at lower wind speeds if dispersant is applied), oil will entrain into the water column, unless it has become too viscous to do so after weathering and the formation of mousse. Once oil is entrained in the water in the form of small droplets, monoaromatics (MAHs) and polynuclear aromatic (PAHs) hydrocarbons dissolve into the water column. The dissolved MAHs and PAHs are the most bioavailable and toxic portion of the oil. The dissolution rate is very sensitive to the droplet size (because it involves mass transfer across the surface area of the droplet), and the amount of hydrocarbon mass dissolved is a function of the mass entrained and droplet size distribution. These are in turn a function of soluble hydrocarbon content of the oil, the amount of evaporation of these components before entrainment, oil viscosity (which increases as the oil weathers and emulsifies), oil surface tension (which may be reduced by surfactant dispersants), and the energy in the system (the higher the energy the smaller the droplets). Large droplets (greater than a few hundred microns in diameter) resurface rapidly, and so dissolution from those is also inconsequential. Dispersant

application facilitates the entrainment of oil into the water in a smaller size distribution than would occur naturally, with the median droplet size about 20 µm (Lunel, 1993a,b).

Thus, the fate of MAHs and PAHs in surface oil is primarily volatilization to the atmosphere, rather than to the water. If wind speeds exceed 12 knots, entrainment of the surface oil into the water becomes significant. Dispersant application can also facilitate entrainment into the water column. If oil is entrained before it has weathered and lost the lower molecular weight aromatics to the atmosphere, dissolved MAHs and PAHs in the water can reach concentrations where they can affect water column organisms or bottom communities (French McCay and Payne, 2001).

Below is a brief description of the physical fates model implemented in SIMAP. Detailed descriptions of the algorithms and assumptions in the model are in published papers (French McCay, 2002, 2003, 2004). The model has been validated with more than 20 case histories, including the Exxon Valdez and other large spills (French and Rines, 1997; French McCay, 2003, 2004; French McCay and Rowe, 2004), as well as test spills designed to verify the model (French et al., 1997).

The three-dimensional physical fates model estimates distribution (as mass and concentrations) of whole oil and oil components on the water surface, on shorelines, in the water column, and in sediments. Oil fate processes included are spreading (gravitational and by shearing), evaporation, transport, randomized dispersion, emulsification, entrainment (natural and facilitated by dispersant), dissolution, volatilization of dissolved hydrocarbons from the surface water, adherence of oil droplets to suspended sediments, adsorption of soluble and semi-soluble aromatics to suspended sediments, sedimentation, and degradation.

Oil is a mixture of hydrocarbons of varying physical, chemical, and toxicological characteristics. Thus, oil hydrocarbons have varying fates and impacts on organisms. In the model, oil is represented by component categories, and the fate of each tracked separately. The “pseudo-component” approach (Payne et al., 1984, 1987; French et al., 1996a; Jones, 1997; Lehr et al., 2000) is used, where chemicals in the oil mixture are grouped by physical-chemical properties, and the resulting component category behaves as if it were a single chemical with characteristics typical of the chemical group.

SIMAP fates model focuses on tracking the lower molecular weight aromatic components divided into chemical groups based on volatility, solubility, and hydrophobicity. In the model, the oil is treated as eight components (defined in Table A-1). Six of the components (all but the two non-volatile residual components) evaporate at rates specific to the pseudo-component. Solubility is strongly correlated with volatility, and the solubility of aromatics is higher than aliphatics of the same volatility, with the MAHs the most soluble, the 2-ring PAHs semi-soluble, and the 3-ring PAHs slightly soluble Mackay et al. (1992a,b,c,d). Both the solubility and toxicity of the non-aromatic hydrocarbons are much less than for the aromatics and dissolution (and water concentrations) of non-aromatics is safely ignored. Thus, dissolved concentrations are calculated only for each of the three soluble aromatic pseudo-components.

TABLE A-1. DEFINITION OF FOUR DISTILLATION CUTS AND THE EIGHT PSEUDO-COMPONENTS IN THE MODEL (MONOAROMATIC HYDROCARBONS, MAHS; BENZENE + TOLUENE + ETHYBENZENE + XYLENE, BTEX; POLYNUCLEAR AROMATIC HYDROCARBONS, PAHS).

Characteristic	Volatile and Highly Soluble	Semi-volatile and Soluble	Low Volatility and Slightly Soluble	Residual (non-volatile and insoluble)
Distillation cut	1	2	3	4
Boiling Point (°C)	< 180	180 to 265	265 to 380	>380
Molecular Weight	50 to 125	125 to 168	152 to 215	> 215
Log(K_{ow})	2.1 to 3.7	3.7 to 4.4	3.9 to 5.6	>5.6
Aliphatic pseudo-components: Number of Carbons	volatile aliphatics: C4 – C10	semi-volatile aliphatics: C10 – C15	low-volatility aliphatics: C15 – C20	non-volatile aliphatics: > C20
Aromatic pseudo-component name: included compounds	MAHs: BTEX, MAHs to C3-benzenes	2-ring PAHs: C4-benzenes, naphthalene, C1-, C2-naphthalenes	3-ring PAHs: C3-, C4-naphthalenes, 3-4 ring PAHs with log(K_{ow}) < 5.6	≥4-ring aromatics: PAHs with log(K_{ow}) > 5.6 (insoluble)

This number of components provides sufficient accuracy for the evaporation and dissolution calculations, particularly given the time frame (minutes) over which dissolution occurs from small droplets and the rapid resurfacing of large droplets (see discussion above). The alternative of treating oil as a single compound with empirically-derived rates (e.g., Mackay et al., 1980; Stiver and Mackay, 1984) does not provide sufficient accuracy for impact analyses because the impacts to water column organisms are caused by MAHs and PAHs, which have specific properties that differ from the other volatile and soluble compounds. Use of more pseudo components does not improve accuracy, as the major constituents of concern are well characterized (sufficiently similar in properties within the pseudo-component group of chemicals) by the modeled component properties used in SIMAP. The model has been validated both in predicting dissolved concentrations and resulting toxic effects, supporting the adequacy of the use of this number of pseudo-components (French McCay, 2003).

The lower molecular weight aromatics dissolve from the whole oil and are partitioned in the water column and sediments according to equilibrium partitioning theory (French et al., 1996a; French McCay 2004). The residual fractions in the model are composed on non-volatile and insoluble compounds that remain in the "whole oil" that spreads, is transported on the water surface, strands on shorelines, and disperses into the water column as oil droplets or remains on the surface as tar balls. This is the fraction that composes black oil, mousse, and sheen.

Lagrangian elements (spillets) are used to simulate the movements of oil components in three dimensions over time. Surface floating oil, entrained droplets, and dissolved components are tracked in separate spillets. Transport is the sum of advective velocities by currents input to the model, surface wind drift, vertical movement according to buoyancy, and randomized turbulent diffusive velocities in three dimensions. The vertical diffusion coefficient is computed as a

function of wind speed in the wave-mixed layer. The horizontal and deeper water vertical diffusion coefficients are model inputs.

The oil (whole and as pseudo-components) separates into different phases or parts of the environment (i.e., surface slicks, emulsified oil (mousse) and tar balls, oil droplets suspended in the water column, dissolved lower molecular weight components (MAHs and PAHs) in the water column, oil droplets adhered and hydrocarbons adsorbed to suspended particulate matter in the water, hydrocarbons on and in the sediments, dissolved MAHs and PAHs in the sediment pore water, and hydrocarbons on and in the shoreline sediments and surfaces). The physical fates model creates output files recording the distribution of a spilled substance in three-dimensional space and time. The quantities recorded are:

- area covered by oil and thickness on the water surface ("swept area");
- volumes in the water column at various concentrations of dissolved aromatics;
- volumes in the water column at various concentrations of total hydrocarbons in suspended droplets;
- total hydrocarbon concentrations and dissolved aromatic concentrations in surface sediment;
- lengths and locations of shoreline impacted and volume of oil ashore in each segment.

The SIMAP model accounts for the presence of ice when calculating surface oil advection, evaporation, entrainment into the water column and surface oil spreading. Table A2 briefly summarizes how the model deals with oil advection and weathering in the presence of different ice concentrations.

TABLE A2: SUMMARY OF OIL-IN-ICE ADVECTION AND WEATHERING EFFECTS ACCOUNTED FOR IN THE SIMAP MODEL.

Ice Cover (Percent)	Advection	Evaporation	Entrainment	Spreading
0 to 30	No change	No change	No change	No change
30 to 80	15° to right	Linear reduction with ice cover	Linear reduction with ice cover	Terminal thickness increased in proportion to ice coverage
80 to 100	Oil moves with pack ice	No weathering	No weathering	Oil thickness computed as a function of ice thickness

References

French, D., M. Reed, K. Jayko, S. Feng, H. Rines, S. Pavignano, T. Isaji, S. Puckett, A. Keller, F. W. French III, D. Gifford, J. McCue, G. Brown, E. MacDonald, J. Quirk, S. Natzke, R. Bishop, M. Welsh, M. Phillips and B.S. Ingram, 1996a. The CERCLA type A natural resource damage assessment model for coastal and marine environments (NRDAM/CME), Technical Documentation, Vol. I - Model Description. Final Report, submitted to the Office of Environmental Policy and Compliance, U.S. Dept. of the Interior, Washington, DC, April, 1996, Contract No. 14-0001-91-C-11.

French, D., M. Reed, S. Feng and S. Pavignano, 1996b. The CERCLA type A natural resource damage assessment model for coastal and marine environments (NRDAM/CME), Technical Documentation, Vol. III - Chemical and Environmental Databases. Final Report, Submitted to the Office of Environmental Policy and Compliance, U.S. Dept. of the Interior, Washington, DC, April, 1996, Contract No. 14-01-0001-91-C-11.

French, D., S. Pavignano, H. Rines, A. Keller, F.W. French III and D. Gifford, 1996c. The CERCLA type A natural resource damage assessment model for coastal and marine environments (NRDAM/CME), Technical Documentation, Vol. IV - Biological Databases. Final Report , Submitted to the Office of Environmental Policy and Compliance, U.S. Dept. of the Interior, Washington, DC, April, 1996, Contract No. 14-01-0001-91-C-11.

French, D.P. and H. Rines, 1997. Validation and use of spill impact modeling for impact assessment. In Proceedings, 1997 International Oil Spill Conference, Fort Lauderdale, Florida, American Petroleum Institute Publication No. 4651, Washington, DC, pp-829-834.

French, D.P., H. Rines and P. Masciangioli, 1997. Validation of an Orimulsion spill fates model using observations from field test spills. In: Proceedings of the Twentieth Arctic and Marine Oilspill Program (AMOP) Technical Seminar, Vancouver, Canada, June 10-13, 1997, Emergencies Science Division, Environment Canada, Ottawa, ON, Canada, pp.933-961.

French McCay, D.P., 2002. Development and Application of an Oil Toxicity and Exposure Model, OilToxEx. Environmental Toxicology and Chemistry 21(10): 2080-2094.

French McCay, D.P., 2003. Development and application of damage assessment modeling: Example assessment for the North Cape oil spill. Marine Pollution Bulletin 47(9-12): 341-359.

French McCay, D.P., 2004. Oil spill impact modeling: Development and validation. Environmental Toxicology and Chemistry 23(10): in press.

French McCay, D. and J.R. Payne, 2001. Model of Oil Fate and Water Concentrations with and without Application of Dispersants. In Proceedings of the 24th Arctic and Marine Oil Spill Program (AMOP) Technical Seminar, Emergencies Science Division, Environment Canada, Ottawa, ON, Canada, pp.611-645.

French McCay, D.P. and J.J. Rowe, 2004. Evaluation of Bird Impacts in Historical Oil Spill Cases Using the SIMAP Oil Spill Model. In Proceedings of the 27th Arctic and Marine Oil Spill Program (AMOP) Technical Seminar, Emergencies Science Division, Environment Canada, Ottawa, ON, Canada, pp. 421-452.

Jones, R.K., 1997. A Simplified Pseudo-Component of Oil Evaporation Model. In Proceedings of the 20th Arctic and Marine Oil Spill Program (AMOP) Technical Seminar, Environment Canada, pp. 43-61.

Lehr, W.J., D. Wesley, D. Simecek-Beatty, R. Jones, G. Kachook and J. Lankford, 2000. Algorithm and Interface Modifications of the NOAA Oil Spill Behavior Model. In Proceedings of the 23rd Arctic and Marine Oil Spill Program (AMOP) Technical Seminar, Vancouver, BC, Environmental Protection Service, Environment Canada, pp. 525-539.

Lunel, T., 1993a. Dispersion: Oil droplet size measurements at sea. In Proceedings of the 16th Arctic Marine Oilspill Program (AMOP) Technical Seminar, Environment Canada, Calgary, Alberta, June 7-9, 1993, pp. 1023-1056.

Lunel, T., 1993b. Dispersion: Oil droplet size measurements at sea. In Proceedings of the 1993 Oil Spill Conference, pp. 794-795.

Mackay, D., S. Paterson and K. Trudel, 1980. A mathematical model of oil spill behavior, Department of Chemical and Applied Chemistry, University of Toronto, Canada, 39 pp.

Mackay, D., W.Y. Shiu and K.C. Ma, 1992a. Illustrated Handbook of Physical-Chemical Properties and Environmental Fate for Organic Chemicals, Vol. I, Monoaromatic Hydrocarbons, Chlorobenzenes, and PCBs. Lewis Publishers, Inc., Chelsea, MI, 668 pp.

Mackay, D., W.Y. Shiu and K.C. Ma, 1992b. Illustrated Handbook of Physical-Chemical Properties and Environmental Fate for Organic Chemicals, Vol. II, Polynuclear Aromatic Hydrocarbons, Polychlorinated Dioxins, and Dibenzofurans. Lewis Publishers, Inc., Chelsea, MI, 566 pp.

Mackay, D., W.Y. Shiu and K.C. Ma, 1992c. Illustrated Handbook of Physical-Chemical Properties and Environmental Fate for Organic Chemicals, Vol. III, Volatile Organic Chemicals. Lewis Publishers, Inc., Chelsea, MI, 885 pp.

Mackay, D., W.Y. Shiu and K.C. Ma, 1992d. Illustrated Handbook of Physical-Chemical Properties and Environmental Fate for Organic Chemicals. Volume IV Oxygen, Nitrogen, and Sulfur containing compounds. Lewis Publishers, Inc., Chelsea, MI, 930 pp.

Payne, J.R., B.E. Kirstein, G.D. McNabb, Jr., J.L. Lambach, R. Redding R.E. Jordan, W. Hom, C. deOliveria, G.S. Smith, D.M. Baxter and R. Gaegel, 1984. Multivariate analysis of petroleum weathering in the marine environment – sub-Arctic , Environmental Assessment of the Alaskan Continental Shelf, OCEAP, Final Report of Principal Investigators, Vol. 21 and 22, Feb. 1984, 690 pp.

Payne, J.R., B.E. Kirstein, J.R. Clayton, Jr., C. Clary, R. Redding, G.D. McNabb, Jr. and G. Farmer, 1987. Integration of suspended particulate matter and oil transportation study. Final Report. Minerals Management Service, Environmental Studies Branch, Anchorage, AK. Contract No. 14-12-0001-30146, 216 pp.

Stiver, W. and D. Mackay, 1984. Evaporation rate of oil spills of hydrocarbons and petroleum mixtures. Environmental Science and Technology 18: 834-840.

Appendix B: Blow-out Model Description

ASA's oil blow-out model is based on the work of McDougall (gas plume model, 1978), Fanneløp and Sjøen (1980a, plume/free surface interaction), and Spaulding (1982) oil concentration model. A simplified integral jet theory is employed for the vertical as well as for the horizontal motions of the gas-oil plume. The necessary model parameters defining the rates of entrainment and spreading of the jet are obtained from laboratory studies (Fanneløp and Sjøen, 1980a). The gas plume analysis is described in McDougall (1978), Spaulding (1982), and Fanneløp and Sjøen (1980a). The hydrate formation and dissociation is formulated based on a unique equilibrium kinetics model developed by R. Bishnoi and colleagues at the University of Calgary. A brief description of the governing equations used in the model and the solution methodology can be found in Spaulding et al. (2000).

In shallow water (< 200 m), oil and gas released from the seabed are driven into the water column as a jet due to the momentum of the discharge. The jet region is confined to the vicinity of the seabed and is relatively short in length (< 1 m). As the discharge moves upward, the density difference between the expanding gas bubbles in the plume and the receiving water result in a buoyant force that drives the plume. The resulting plume is analogous to a thermal plume, with the important exception that for blow-outs, the plume is bubble-starved, because the bubbles are few in number and large. The presence of the bubbles leads to a two-layer structure, with an inner core bubble plume and an outer ring of mostly entrained water. As the plume rises, it continues to entrain ambient sea water due to the velocity difference between the rising plume and the receiving water. This entrainment reduces the plume's velocity and buoyancy and increases its radius. The oil in the release is rapidly mixed by the turbulence in the rising plume, causing it to break up into small droplets. These droplets (typically a few micrometers to millimeters in diameter) are rapidly transported upward by the rising plume, their individual rise velocities contributing little to their upward motion. As the plume reaches the sea surface, it is deflected in a radial surface flow zone without appreciable loss of momentum. This radial jet, with its origin at the surface directly above the blow-out, carries the oil particles rapidly away from the center of the plume. The velocity and oil concentrations in this surface flow zone decrease while the depth of the zone increases. Finally, in the far-field, where the plume buoyancy has been dissipated, ambient currents and wind generated waves determine the subsequent transport and dispersion of the oil.

There are several important modifications that may alter this basic description of jet/plume behavior. If the buoyant driving force for the plume is dissipated by entrainment before it reaches the surface, the oil droplets in the plume will be carried to the surface solely by their own rise velocities and the surface interaction zone will effectively disappear. The plume behavior can also be altered by variations in the ambient density field, which can cause trapping of the plume in the water column. Finally, in the presence of ambient currents, the plume path can be substantially altered as the current forces the jet to bend from its preferred vertical direction. If the current velocity profile with depth varies with time, the path of the plume can become very complicated.

As water depths become deeper (> 200 m), the basic dynamics of the oil/gas jet/plume become more complicated, principally due to the increase in hydrostatic pressure at the seabed, which leads to the possibility of the formation of gas hydrate solids. Gas hydrates constitute a class of solids in which small molecules occupy almost spherical holes in ice-like lattices made up of hydrogen-bonded water molecules. This class of solids is known as clathrates. Clathrate compounds are characterized by the structural combinations of two substances that remain associated not through strong attractive forces, but because strong mutual binding of the molecules of one sort makes possible the firm enclosure of the other. The hydrate-forming gases include light alkanes, carbon dioxide, hydrogen sulphide, nitrogen, and oxygen. Gas hydrates can exist in one of four structures; Structure I and Structure II, Structure H and a new, as of yet unnamed structure. Methane, the most typical gas likely to be released during a blow-out, is known to form Structure I hydrates. A portion or the entire volume of released gas may be converted to hydrates. These hydrates, which typically form on the gas bubbles close to the release location, have specific gravities on the order of 0.92 to 0.96. The hydrate solids break into small particles and are transported by their rise velocity and the ambient currents. The conversion of the gas into gas hydrates, to the extent that it occurs, deprives the plume of its principal source of buoyancy, leaving the oil droplets and gas hydrates free to rise under the action of their own buoyancy. The oil and gas hydrates in this much less vigorously mixed plume may be carried over very large distances in the water column before ultimately reaching the sea surface.

A review of the literature shows that our understanding and ability to model the dynamics of rising oil and gas plumes in shallow water is extensively developed. Early work by Fannelop and Sjoen (1980a,b), Spaulding (1982), and Milgram (1983), using integral plume theory, has been extended by Rye (1994) and Kolluru (1993) into operational models to predict plume dynamics and oil concentrations. Zheng and Yapa (1997a,b, 1998) have further developed and refined this basic approach for buoyant oil jets and smoke plumes. Their model has been extensively tested against analytic and theoretical results and laboratory and field experiments. Rye (1996) and Rye et al. (1996) describe a 1995 experiment in the North Sea. In all cases, the models performed well against theory and field observations. They also correctly predicted the height of the transition zone from when oil transport was dominated by plume dynamics to when oil droplet rise velocities dominated its movement.

The most critical issue for deepwater blow-outs is the formation rate of gas hydrates under the gas/oil flow rates, hydrostatic pressures, temperatures, and salinity at typical blow-out sites. Topham (1977) performed field experiments using simulated natural gas at a release depth of 650 m, with and without oil, and observed the formation of hydrates in both cases. He was unable to determine the rates of formation but did note that hydrates did not form at depths shallower than about 300 m. Bishnoi and Mainik (1979) performed a set of laboratory experiments using a high pressure test facility (2,000 psi) (equal to a seawater depth of 1,370 m). According to their work, gas-to-hydrate conversion was complete when starting pressures were in excess of 700 psi (480 m) and ceased when the pressure was lower than 450 psi (310 m). It is noted that the hydrate formation pressures are highly dependent on the gas or hydrocarbon liquid compositions. For very light condensate oils or rich gases, the

pressure could be even lower than 450 psi. Quantitative estimates of the rates were not provided. Zheng and Yapa (1999) have recently extended their model to include a very simplified hydrate formation component. The approach ignores the kinetics of hydrate formation, assumes that all hydrates are formed at the very beginning of the release, and that the conversions are based on ideal gas laws.

References

Bishnoi, P.R. and B.B. Mainik, 1979. Laboratory study of behaviour of oil and gas particles in salt water, relating to deepwater blow-outs. Spill Technology Newsletter 4(1): 24-36.

Bishnoi, P.R., A.K. Gupta, P. Englezos, N. Kalogerakis, 1989. Multiphase equilibrium flash calculations for systems containing gas hydrates. Fluid Phase Equilibria 53: 97-104.

Fanneløp, T.K. and K. Sjoen, 1980a. Hydrodynamics of underwater blow-outs. AIAA 8th Aerospace Sciences Meeting, January 14-16, Pasadena, California, AIAA paper, pp. 80-0219.

Fanneløp, T.K. and K. Sjoen, 1980b. Hydrodynamics of underwater blow-outs. Norwegian Maritime Research 4: 17-33.

Kolluru, V., M.L. Spaulding and E. Anderson, 1993. Application and verification of WOSM to selected spill events, 16th Arctic and Marine Oil Spill Program (AMOP), Technical Seminar, June 7-9, 1993, Calgary, AB, pp. 647-668.

McDougall, T.J., 1978. Bubble plumes in stratified environments. Journal of Fluid Mechanics, 85(4) 655-672.

Milgram, J.H., 1983. Mean flow in round bubble plumes. Journal of Fluid Mechanics 133: 345-376.

Rye, H., 1994, Model for calculation of underwater blow-out plume. Proceedings of the 17th Arctic and Marine Oilspill Program (AMOP), Technical Seminar, Canada, p. 849-865.

Rye, H., 1996. NOFO exercise 1995. Dispersants and underwater release experiments-Observations and modelling of the underwater plume behaviour. Data report", IKU Report No.41.514.00/03/95 dated 19 January.

Rye, H., P. Brandvik and M. Reed, 1996, Subsurface oil release field experiment - Observations and modeling of subsurface plume behavior. Proceedings of the 19th Arctic Marine Oilspill Program (AMOP), Technical Seminar, Calgary, AB, pp 1417-1435.

Spaulding, M.L., 1982. User's manual for a simple gas blow-out plume model. Continental Shelf Institute, Trondheim, Norway.

Topham, D.R., 1977. Observations of the formation of hydrocarbon gas hydrates at depth in seawater. Spill Technology Newsletter, July-August, 2(4) 23-28.

Yapa, P.D. and L. Zheng, 1997b. Simulation of oil spills from underwater accidents - I: Model development. International Association of Hydraulic Research, The Netherlands, Journal of Hydraulic Research 35(5). 673-688.

Zheng, L. and P. Yapa, 1997a, A numerical model for buoyant oil jets and smoke plumes. Proceedings of the 20th Arctic Marine Oilspill Program (AMOP), Technical Seminar, Vancouver, BC, pp. 963-979.

Zheng, L. and P.D. Yapa, 1998. Simulation of oil spills from underwater accidents II: Model verification. International Association of Hydraulic Research, The Netherlands, Journal of Hydraulic Research 36(1): 117-134.

Zheng, L. and P.D. Yapa, 1999. A deepwater jet/plume model and a parametric analysis. Proceedings of the 22nd Arctic and Marine Oilspill Program (AMOP) ,Technical Seminar. Calgary, AB. pp. 285-299.